Electromagnetic Torque From Event Report Data – A Measure of Machine Performance

Dale Finney and Derrick Haas

Schweitzer Engineering Laboratories, Inc.

For the complete history of this paper, refer to the next page.

Electromagnetic Torque From Event Report Data – A Measure of Machine Performance

Dale Finney and Derrick Haas, *Schweitzer Engineering Laboratories, Inc.*

Abstract—**Power system events (such as starting a motor), a fault on the motor supply, or a switching event (such as the transfer of a motor from a primary to an alternate source) all expose a motor to transients. The electromagnetic torque response can be used as a measure of the impact of an event on the motor. A very large torque during a switching event can help identify improper switching controls or even the need to inspect a motor for damage. Motor torque calculated during normal motor starts and transfers can be trended to identify developing problems.**

While measuring the mechanical torque on the shaft of the machine can be challenging, it is possible to calculate the electromagnetic torque or air-gap torque directly from the motor terminal voltage and stator current. This paper discusses how electromagnetic torque can be calculated from oscillographic event report data obtained from digital motor protection. Several example cases are shared.

I. INTRODUCTION

In 1990, Ojo published the results of an Electric Power Research Institute-sponsored study that describes several methods for calculating torque pulsations from terminal measurements for synchronous motors during starting [1]. The calculated values were compared with measurements on a test motor with good results. In this paper, we focus on the modified volt-second-ampere (MVSA) method. The method is generally applicable to induction machines and can be used to accurately calculate instantaneous torque for a wide variety of events, including an external fault or a motor bus transfer. The calculations are simple enough to implement in a spreadsheet or similar software tool. Using this method, data captured from a motor start can be used to calculate the electromagnetic torque produced by the motor. These data can then be compared with torque transients from other events.

II. CALCULATING ELECTROMAGNETIC TORQUE FROM ELECTRICAL QUANTITIES

To understand the basis of the MVSA method, we refer to the general equations for an induction machine in the direct-quadrature-zero (DQ0) reference frame [2] [3].

$$v_{qs} = R_S \cdot i_{qs} + \frac{\omega}{\omega_b} \cdot \psi_{ds} + \frac{p}{\omega_b} \psi_{qs} \tag{1}$$

$$v_{ds} = R_S \cdot i_{ds} - \frac{\omega}{\omega_b} \cdot \psi_{qs} + \frac{p}{\omega_b} \psi_{ds} \tag{2}$$

$$v_{0s} = R_S \cdot i_{0s} - \frac{p}{\omega_b} \cdot \psi_{0s} \tag{3}$$

$$v_{ds} = R_R \cdot i_{qr} + \frac{\omega - \omega_r}{\omega_b} \cdot \psi_{dr} + \frac{p}{\omega_b} \psi_{qr} \tag{4}$$

$$v'_{dr} = R_R \cdot i_{dr} - \frac{\omega - \omega_r}{\omega_b} \cdot \psi_{qr} + \frac{p}{\omega_b} \psi_{dr} \tag{5}$$

$$v'_{0r} = R_R \cdot i_{0r} - \frac{p}{\omega_b} \cdot \psi_{0s} \tag{6}$$

$$T_e = \psi_{ds} \cdot i_{qs} - \psi_{qs} \cdot i_{ds} \tag{7}$$

In (1) through (7) v, i, and ψ are instantaneous values of voltage, current, and flux linkage, respectively; r is resistance; and p is the derivative operator. All quantities are in per unit (pu). The subscripts d, q, and 0 refer to direct-, quadrature-, and zero-axis quantities. The subscripts s and r refer to stator and rotor quantities. Finally, ω is the radian frequency of the reference frame, ω_r is the radian frequency of the rotor, and ω_b is the base radian frequency. We include all seven equations for completeness; however, we use only (1), (2), and (7). Note that the flux linkage is in terms of reactance rather than inductance.

In this section, we work with DQ0 quantities because this is how machine equations are presented in most references. Later in the paper, we carry out the MVSA calculations using abc quantities because this saves several processing steps.

Equation (7) gives the equation for electromagnetic or air-gap torque. Under steady-state conditions, the terms on the right-hand side of (7) are symmetrical sinusoids, and T_e is a constant component. We may consider how a constant torque can result from a calculation that uses sinusoidal inputs. On the right-hand side, we subtract two products. Now, when we take the product of two sinusoids, the result is a double-frequency sinusoid with a dc offset. During the subtraction, if the ac components of the two products have equal magnitudes and are in phase, then we will be left with pure dc. By definition, d-axis and q-axis quantities are 90 degrees apart. As we will see later in this section, if we neglect r_s momentarily, flux linkage is the time-integral of voltage. In the steady state, this translates into a 90-degree phase shift. We conclude that the two product terms in (7) are in phase during the steady state.

We can use a DQ0 transformation to directly calculate the stator currents i_{qs} and i_{ds} in (7) from the motor terminal current, i_{abc} [2]. However, the flux linkages (ψ_{ds} and ψ_{qs}) are not directly available. Rearranging (1) and (2) we get:

$$p\psi_{qs} = \omega_b \bullet v_{qs} - \omega_b \bullet R_S \bullet i_{qs} - \omega \bullet \psi_{ds} \tag{8}$$

$$p\psi_{ds} = \omega_b \bullet v_{ds} - \omega_b \bullet R_S \bullet i_{ds} + \omega \bullet \psi_{qs} \tag{9}$$

The terms $\omega \bullet \psi ds$ and $\omega \bullet \psi qs$ in (8) and (9) are often called the speed voltages. They are a general consequence of transforming an inductance from the abc frame to the DQ0 frame. Physically, they represent a cross-coupling between the q and d axes. The speed voltage term in each equation contains ω. This value is in per unit and is zero in the steady state (i.e., when the reference frame is stationary) and close to zero otherwise. If we turn now to the first two product terms on the right-hand side of (8) and (9), we see that both terms contain ω_b. This term has a value of 377 radians per second in a 60 Hz system. Because $\omega_b \gg \omega$, the speed voltages can safely be dropped from (8) and (9). This simplifies the calculations with virtually no loss in fidelity. For this paper, we carry out a large number of simulations to confirm this assertion.

We can now rewrite (8) and (9) as:

$$\psi_{ds} = \omega_b \bullet \int (v_{ds} - R_s \bullet i_{ds}) \tag{10}$$

$$\psi_{qs} = \omega_b \bullet \int (v_{qs} - R_s \bullet i_{qs}) \tag{11}$$

In (10), v_{qs} and v_{ds} can be directly calculated using Vabc measured at the motor terminals and a DQ0 transform; i_{qs} and i_{ds} are obtained in a similar manner. The only required motor parameter is stator resistance R_S, and this value can be obtained from the manufacturer's data or be directly measured with the machine offline. If it is an older motor, R_S may not be readily available. Rotor speed is not needed.

A. Integration to Determine Flux Linkage

In (10), we see that integration is required. Because we are working with instantaneous values from an event record, we need to do numerical integration. Here we can use the trapezoidal rule. The general form of this equation is shown in

(12), where h is the time difference between samples and i is a sample index.

$$\int_i^{i+1} f(i) = \frac{h}{2}(f(i) + f(i+1)) \tag{12}$$

When calculating torque for a transient event, we assume that we begin from a steady state. This means our event record begins with prefault data. In the steady state, we do not expect the flux linkages (ψ_{ds} and ψ_{qs}) to have a dc component. However, because the event record begins at an arbitrary instant in time, the random start of integration will likely introduce a dc component that must be removed. One way to do this is to start integrating at a peak of the signal phi. Another is to calculate the dc component in the prefault calculated flux and subtract it from the entire calculation.

$$\psi_{ds} = \omega_b \bullet \int (v_{ds} - R_S \bullet i_{qs}) - DC_d \tag{13}$$

$$\psi_{qs} = \omega_b \bullet \int (v_{qs} - R_S \bullet i_{qs}) - DC_q \tag{14}$$

Here DC_d and DC_q are one-cycle averages from the prefault data given by (15) and (16), where n is the number of samples in one cycle of data.

$$DC_d = \Sigma_{i=0}^n \frac{\psi_{dsi}}{n} \tag{15}$$

$$DC_q = \Sigma_{i=0}^n \frac{\psi_{qsi}}{n} \tag{16}$$

The process is equivalent to finding a constant of integration.

Finally, torque is calculated using the values of ψ_{ds} and ψ_{qs} calculated from (10), and i_{ds} and i_{qs} from (7).

In Fig. 1, we show a model of a 1,000 horsepower (hp) motor connected to a power system through a circuit breaker. The model parameters are given in the appendix. During model execution, we open the breaker, allow the motor to run down, then reclose the breaker when the angle across the breaker has reached a specified value. This sequence exposes the motor to a torque transient. The air-gap torque is available as a state variable from the model.
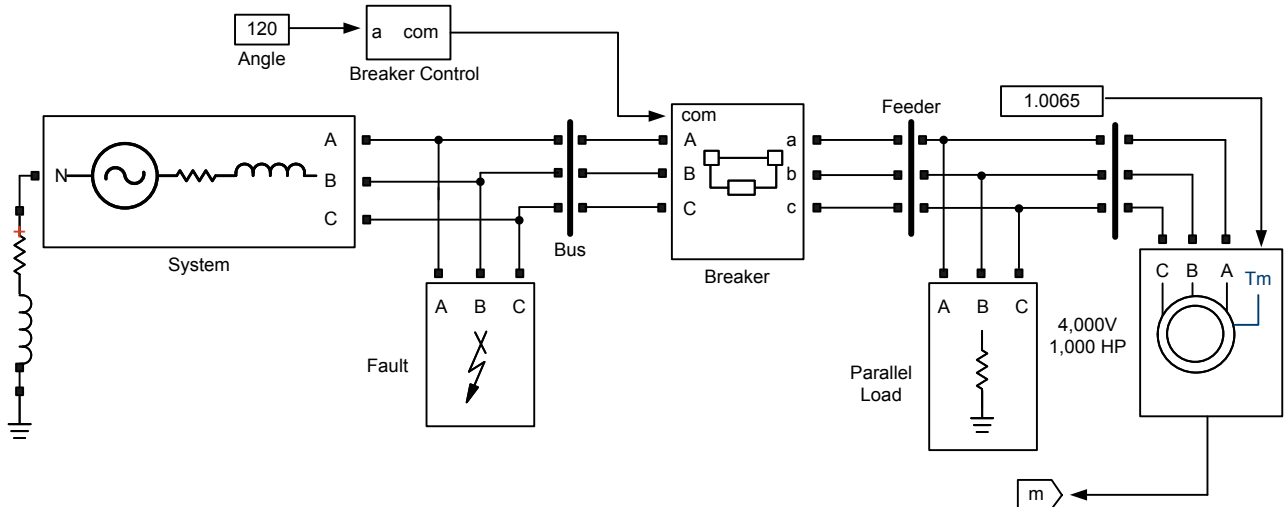

Fig. 1.   Simulink Model

Fig. 2 shows the results of a simulated motor start for the model of Fig. 1. The red trace shows the torque produced by the model, and the yellow is the torque calculated using the previously described method.
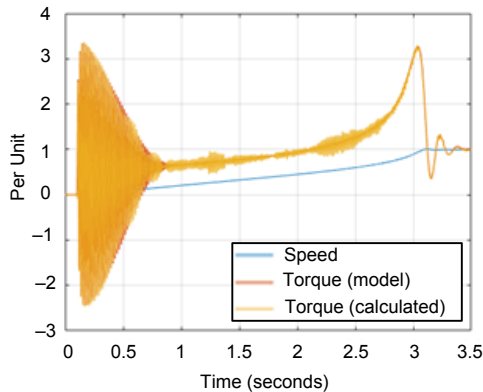

Fig. 2.   Simulated Motor Start at t = 0 Seconds

We can investigate the impact of initialization with the help of our model. In Fig. 3 and Fig. 4, we show the errors introduced in the calculation if the integration is not correctly initialized. Fig. 3 compares the calculated and actual values of ψ_{qs}. A significant dc component is evident.
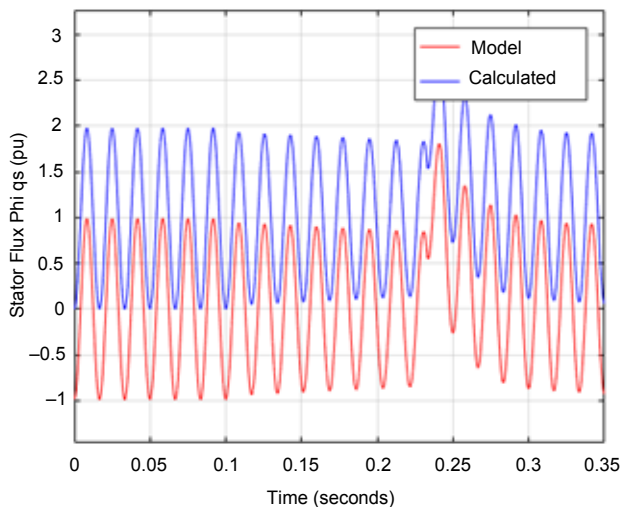
Fig. 3.   Flux Error Resulting From Incorrect Initialization

In fact, integration was started at a zero crossing of the signal ψ_{qs} in this example, giving the worst-case error in the dc term.

The dc offset in the calculated ψ_{qs} is manifested as a ripple in the prefault torque calculation shown in Fig. 4.

Normally, we will have nothing with which to compare our calculation. However, because we expect a constant torque in

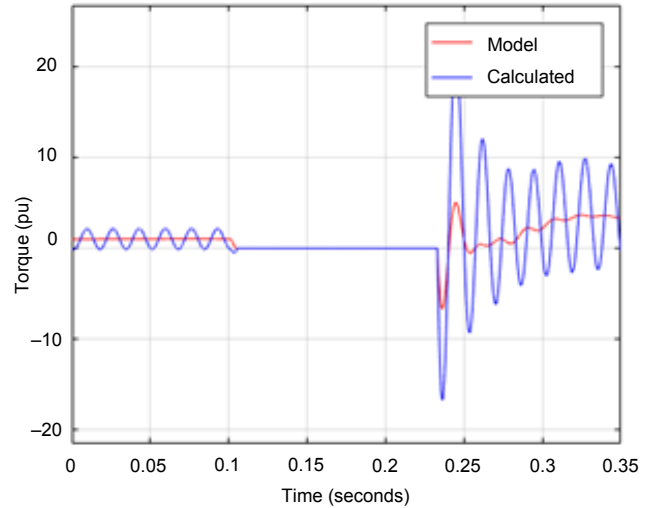the prefault, this observed ripple is a very good indication of an integration problem.

Fig. 4.   Torque Error Resulting From Incorrect Initialization

B.   Impact of Sampling Rate

Because we are interested in calculating torque from an event capture, it is useful to look at the impact of sampling rate on the accuracy of the calculation. We begin again with the model of Fig. 1 and downsample the voltage and current to 16 and 8 samples per cycle (SPC) before the torque calculation. These rates are representative of those commonly available in digital motor protection relays. Fig. 5 shows the torque from the model plotted against the calculated values using each sampling rate. Note that the results are very good.
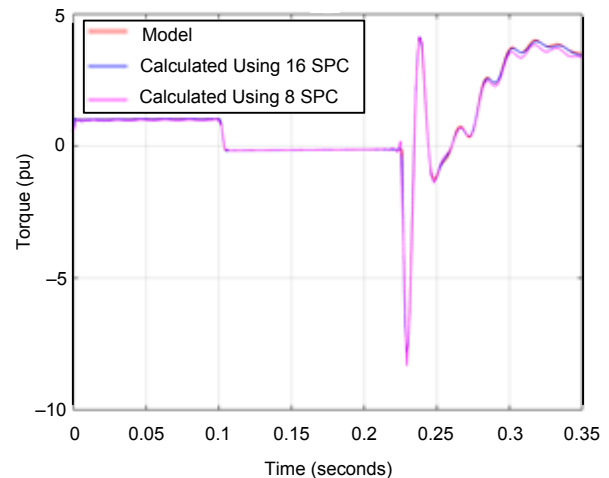

Fig. 5.   Torque Error Resulting From Downsampling

Fig. 6 is a close-in view of the first peak. For this event, the error in peak torque at the first peak is 1.6 percent at 16 SPC and 8.1 percent at 8 SPC.
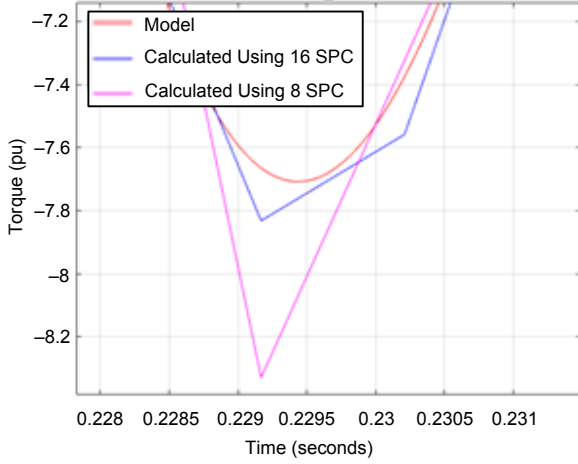

Fig. 6.   Close-In View of the First Peak in Fig. 4

C.   Impact of Stator Resistance

Next, we consider the impact of stator resistance. This is the only motor parameter that impacts the torque calculation. It is relatively easy to obtain and does not vary with motor speed. However, it does have a temperature dependence. The temperature coefficient of copper (α) is $3.9 \cdot 10^{-3}$ per degree Celsius. If we consider a worst-case temperature rise of 55°C, we can calculate the resistance change as follows:

$$\frac{\Delta R_S}{R_{amb}} = \alpha \cdot \Delta T = 3.9 \cdot 10^{-3} \cdot 55 = 21.5\% \qquad (17)$$

Our model of Fig. 1 has a stator resistance of 0.01117 pu. In Fig. 7, we show an event and the corresponding model torque where the stator resistance has increased by 21.5 percent, compared with a calculated torque where the resistance at ambient is used and a calculated torque where resistance is not included at all ($R_S = 0$).

We can make several observations. In the prefault, there is no ripple in either calculated value. This is because the current is small. Comparing the calculated and model post-fault values, we note a sustained 60 Hz ripple that is not evident in the model torque. Both calculated values are relatively accurate for the first peak, but the errors are much larger thereafter. For this event, the error in peak torque at the first peak is −1.8 percent using $R_S = R_{amb}$ and −10 percent for $R_S = 0$.
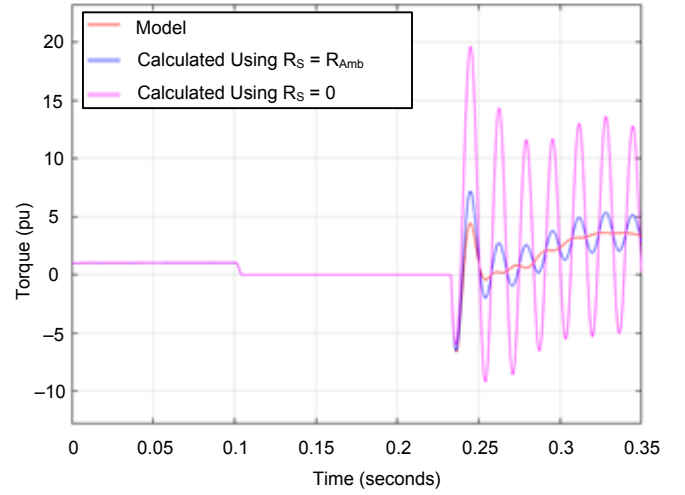

Fig. 7.   Torque Error Resulting From Incorrect Stator Resistance

The protective relay that captured the event may also measure the motor temperature. In this case, the measured temperature could be used along with (17) to correct the resistance and thereby improve the calculation accuracy.

D.   Impact of Current Transformer (CT) Saturation

We investigated the impact of CT saturation by adding a C200 CT and C100 CT to the model. The details of the CTs are shown in Table III of the appendix. Fig. 8 compares the calculated torques using each CT with the model value.
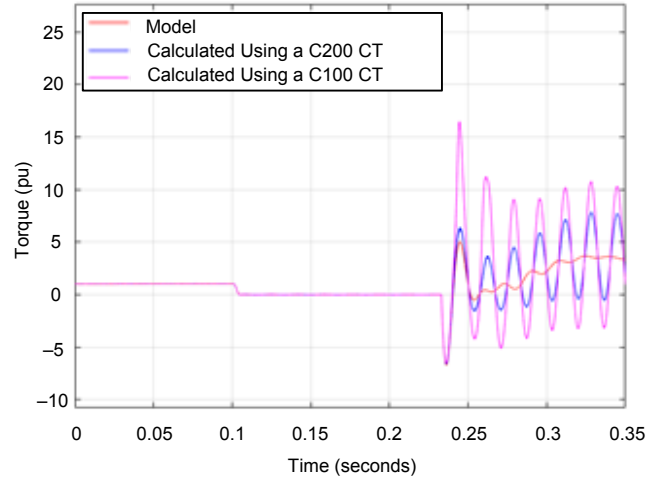

Fig. 8.   Torque Error Resulting From CT Saturation

Note that both calculated values are accurate at the first peak but overestimate the value of subsequent peaks.

In Fig. 9, we show the A-Phase currents for this test. This phase had the high peak magnitude and the largest degree of CT saturation. We can see that both the C200 and C100 CTs do a reasonable job in the first half cycle but later in the event, CT saturation acts to attenuate the dc component. This has a big impact on the torque calculation later in the event. Inspection of the waveforms can usually identify significant CT saturation.
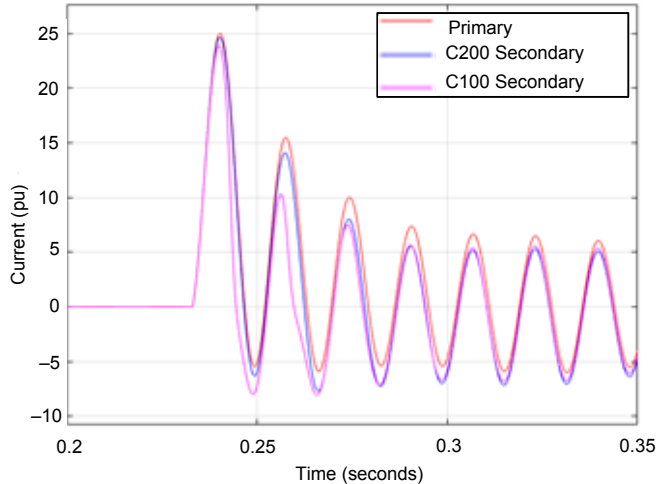

Fig. 9.   Current During CT Saturation on A-Phase

E.   Impact of Core Saturation

We now turn to saturation of the iron core in the motor itself; namely, the iron in both the stator and rotor. We applied the saturation curve of Fig. 10 to the model.
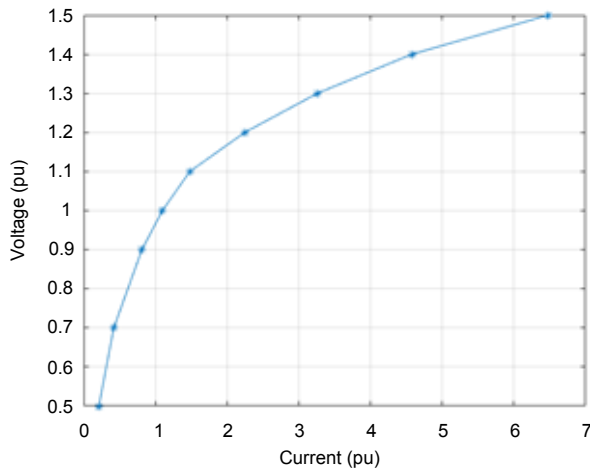

Fig. 10.   Saturation Curve for the Model of Fig. 1

Fig. 11 shows the simulation results. We see that core saturation does have a small impact. The error in the first peak is 3.6 percent.
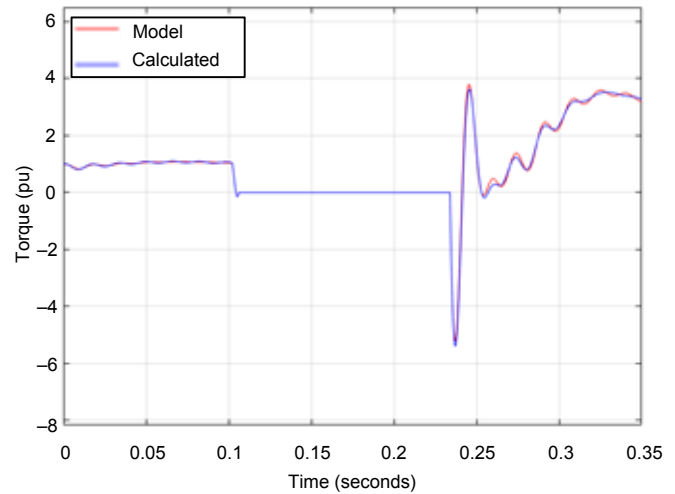

Fig. 11.   Errors Resulting From Core Saturation

F.   Total Errors

In the previous analysis, we showed individual impacts on the accuracy of the torque calculation. As a final test, we included all factors described previously and ran a batch of cases for two types of events: faults at the machine terminals (128 cases) and out-of-phase reclose events (180 cases). For faults, we varied the load, the point-on-wave, the fault type, and the fault resistance. For out-of-phase reclosing, we varied the load and the reclose angle. Earlier we noted that resistance errors could be significant. We therefore ran the test for two values. The results are shown in Table I. Note that the maximum error can exceed 40 percent. The cases with the largest errors are primarily those that have CT saturation in the first half cycle. As shown in Fig. 8, CT saturation tends to cause torque overestimation.

TABLE I
FIRST PEAK AVERAGE AND MAXIMUM TORQUE ERRORS
INCLUDING ALL FACTORS

Stator Resistance Error (%)	First Peak Torque Error (%)			
	Terminal Faults		Out-of-Phase Reclosing	
	Avg	Max	Avg	Max
5	3.76	41.1	2.33	21.84
20	3.86	41.4	6.77	45.37

IV. EXAMPLES

In the previous section, we used simulations to characterize sources of error. In this section, several real-world cases are analyzed. For these events, the electromagnetic torque results shared were calculated using the phase quantities rather than DQ0 quantities. Note that the results are the same for both cases, but for the sake of brevity, we only share the results of the calculation based on the phase currents and voltages. As pointed out in Section I, the equations were provided as DQ0 quantities to match the existing published literature and most motor analysis texts. Calculating torque using the phase quantities directly is computationally more efficient because it does not require any transformations from phase to DQ0 quantities.

A. Example I—Start of 2,500 hp Motor

This example is a medium voltage 2,500 hp motor during a normal start. A simplified version of the single-line diagram is shown in Fig. 12.
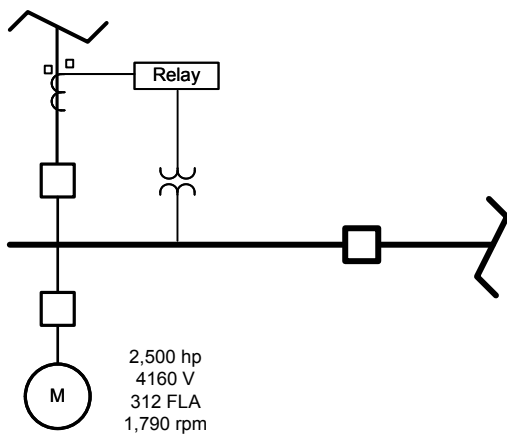

Fig. 12.   Simplified Single-Line Diagram for Example I

This particular event report is a lower resolution event report, only four SPC, as compared with the 8 and 16 SPC plots shown in the simulations in Section II. We also do not have the stator resistance for this machine. The stator resistance at a particular temperature is often readily available in the motor data sheets. This particular motor has a limited amount of documentation available. While this could be easily measured or obtained, scheduling an outage of this machine to measure the winding resistance is impractical. In addition, it is worth noting that the voltage measurement location is not directly at the motor terminals. There is a length of medium-voltage cable between the switchgear and the motor. This cable impedance should be accounted for by adding the cable resistance to the resistance of the stator winding and using the combined impedance in the torque calculation. We therefore assume a value of 0.01 pu and will look at how large of an impact adjusting that value will have on calculating the starting torque. The torque is shown in Fig. 13.
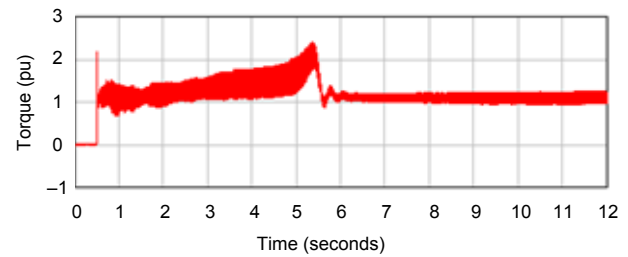

Fig. 13.   Torque During Starting With Evident Errors

We can vaguely make out a jump in torque around 0.5 seconds followed by a ramp in torque until it reaches a peak at around 5.5 seconds, with a sharp dropoff as the motor gets up to speed at around 6 seconds. However, there are heavy oscillations and ringing, even after the machine has come up to speed. If we take a closer look at the flux signals, particularly the A-Phase flux in Fig. 14, we see a noticeable linear decay as the event goes on. We are looking at a sinusoidal flux; however, because of the timescale of the event, the oscillations look like a shaded area. We can see the average of the sinusoidal flux is around 0 pu at the beginning of the event report but slowly decreases to nearly –0.5 pu at 12 seconds.
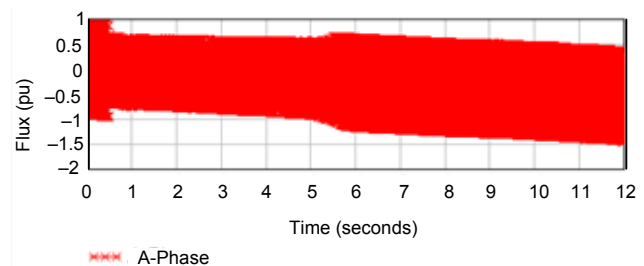

Fig. 14.   Linear Decrease of A-Phase Calculated Flux

A closer look at the voltage signals reveals the presence of a very small amount of dc (less than 1 percent of the 60 Hz component). Integrating a dc component results in a linear offset in the flux waveforms. This dc is not found in any simulations, and realistically it should not be present in the ac power system and should be considered noise. Even if there were pure dc voltage present on the power system, the potential transformers (PTs) would not be able to measure it. The source of this dc could be from the electronic circuits in the relay itself. Relay manufacturers do typically calibrate relays to remove any standing dc, and some relays use the presence of dc in a waveform as an indication of a problem with the relay. Scaling and event conversion could have presented some errors as well.

Lastly, it is worth noting again that the sampling rate of this event is very low at just four SPC. Ideally, an event report with a higher sampling rate should be used (at least eight SPC) per the analysis done in Section II. Fig. 15 shows the A-Phase flux after the dc voltage in A-Phase has been removed.
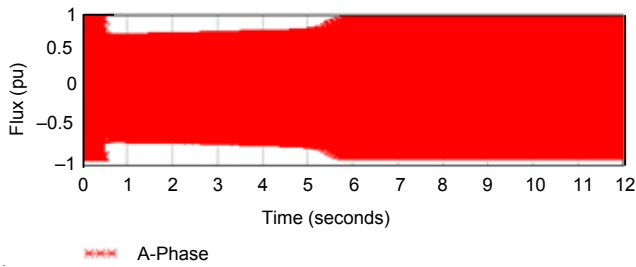
Fig. 15. A-Phase Flux After Removal of DC Voltage

The resulting torque is shown in Fig. 16. The blue trace represents the torque after removal of dc, whereas the red trace is the same torque signal from Fig. 13 plotted for comparison.

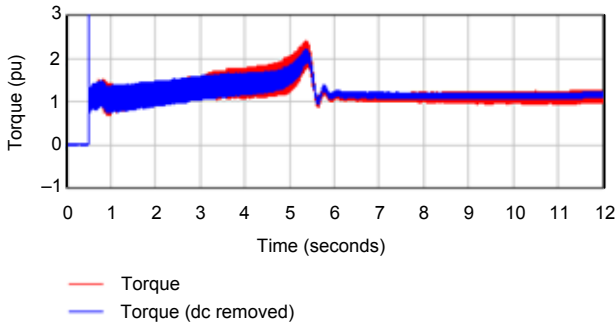

Torque
Torque (dc removed)

Fig. 16. Torque With and Without DC Removed From Voltage Signals

Overall in Fig. 16, we can see that removing the dc resulted in fewer oscillations and a torque that is more representative of what we expect for motor torque during a start. Fig. 17 shows the impact of varying the stator resistance, with three values of stator resistance plotted, just to show the overall impact on the torque calculation. Unlike our switching event shown in the previous section, varying the stator resistance has a large impact on the motor start event and calculation of torque throughout the motor start.
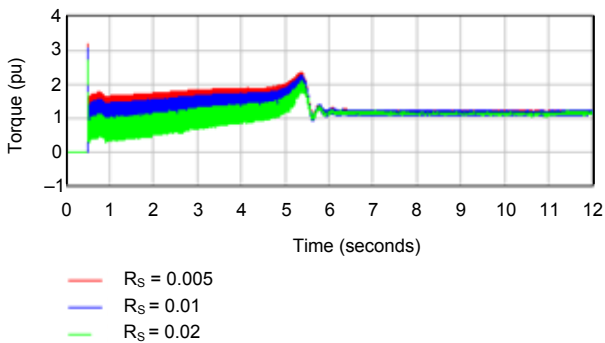

$R_S = 0.005$
$R_S = 0.01$
$R_S = 0.02$

Fig. 17. Impact of Starting Torque With Varying Stator Resistance

B. Example II—Motor Bus Transfer in Lab

This next example is from a staged reclose on a small 10 hp motor in a university lab. A simplified single-line diagram of the motor and connected system is shown in Fig. 18. The motor was loaded at approximately half of rated mechanical load during the switching event. The contactor closed on the motor

when the motor residual voltage and the supply voltage were approximately 90 degrees out of phase. The small motor physically "jumped" during the severe switching event. While many of the machine parameters for this motor are known, the stator resistance was not known at the time of the test.
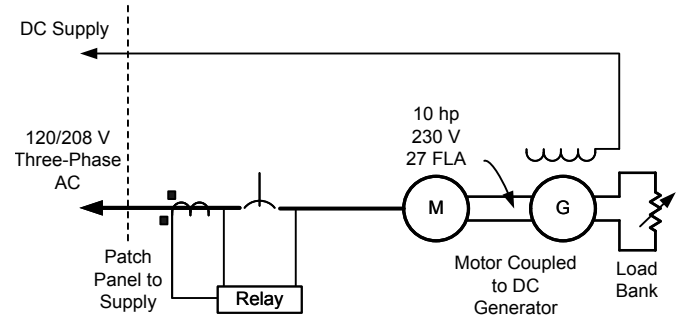

Fig. 18. Simplified Single-Line Diagram

The calculated motor torque is shown in Fig. 19, and a closer look at the time period around the switching event around (0.2 seconds) is shown in Fig. 20.
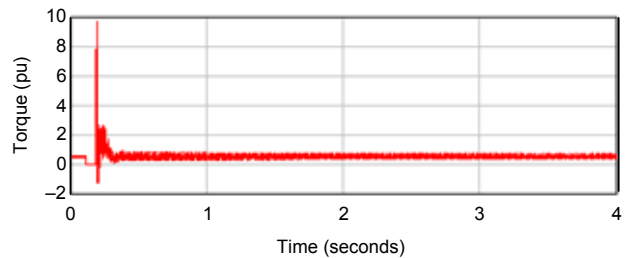

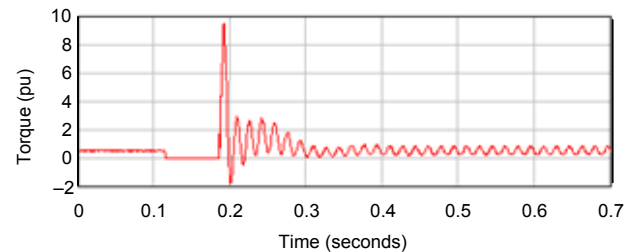Fig. 19. Motor Torque During Reclose

Fig. 20. Close-In View of Fig. 19

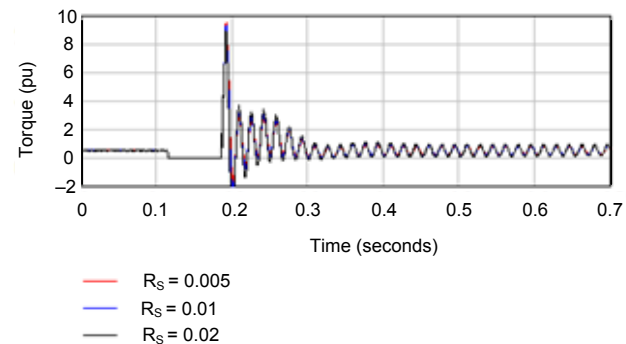If we vary the stator resistance as before, we can see the results in Fig. 21 and a closer look in Fig. 22.

$R_S = 0.005$
$R_S = 0.01$
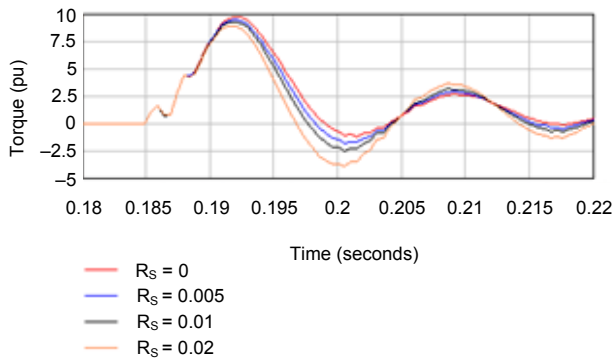$R_S = 0.02$

Fig. 21. Torque vs. R_S

Fig. 22.   Closer Look at Motor Torque vs. R_S

The initial peak torque values following the switching event are all very close regardless of which value of stator resistance we use. The maximum is 9.74 pu with R_S at 0, and the minimum is 8.96 pu with R_S at 0.02 pu. Knowing the exact value of stator resistance or measuring it can help narrow down more precisely how much air-gap torque is produced during this event.

This out-of-phase reclose on the motor caused a tremendous amount of stress on the small machine. It should also be noted that removal of dc from the voltage signals was not required in this case—only a removal of the "dc flux" to properly initialize the integration.

C.   Example III—Real-World Motor Bus Transfer

This last example involves an event report captured during the transfer of a 13.8 kV auxiliary bus in a power plant from the primary to an alternate source. The load of a 1,750 hp induction motor was transferred. The event report was a 16 SPC resolution event, where the voltages were from an open-delta PT connection. As shown in the appendix, the torque equation can be calculated from phase-to-phase voltages. A result of the torque calculation is shown in Fig. 23. Like all of our examples, the stator resistance is an unknown quantity for this motor, so a value of 0.01 pu for R_S is assumed again.
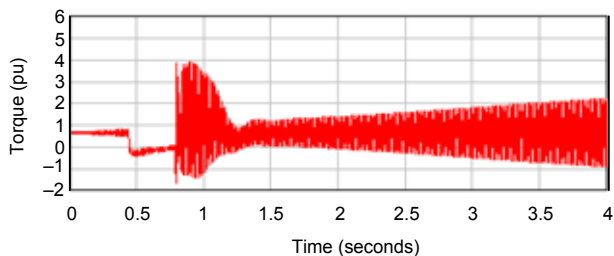

Fig. 23.   Motor Torque During Auxiliary Bus Transfer

Like in Example I, there is a large amount of oscillation in the calculated torque during the preswitching or prefault portion of the event. If we take a closer look at the flux signals (in particular, the flux calculated for the VAB voltage in Fig. 24), we notice a linear decay. This is because there is a small dc component present in the voltages measured by the relay. Just as before, if we remove the dc component of the voltages, we end up with a calculated torque in Fig. 25.
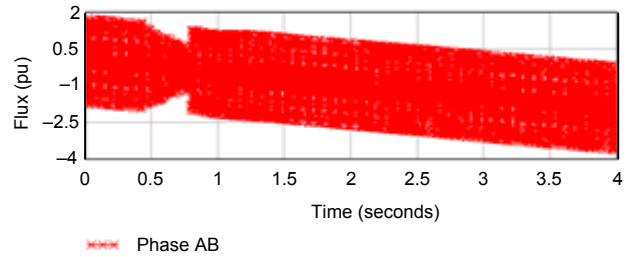

Phase AB

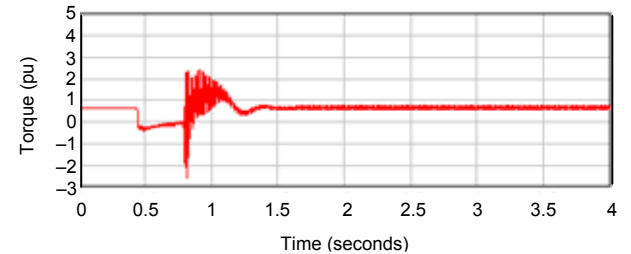Fig. 24.   Calculated Flux From VAB

Fig. 25.   Motor Torque From Auxiliary Bus Transfer After Removing DC

As before, we can adjust the assumed value of R_S to see its impact on the torque calculation in Fig. 26 and take a closer look in Fig. 27.
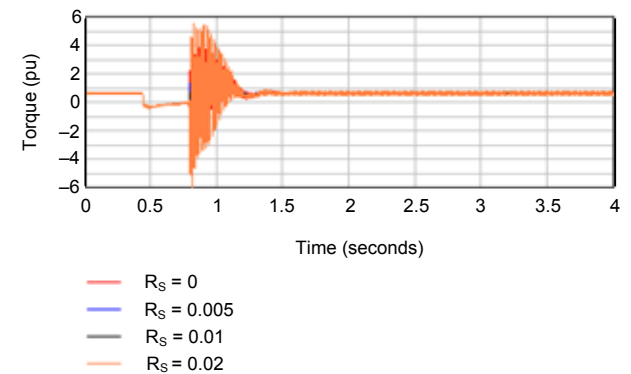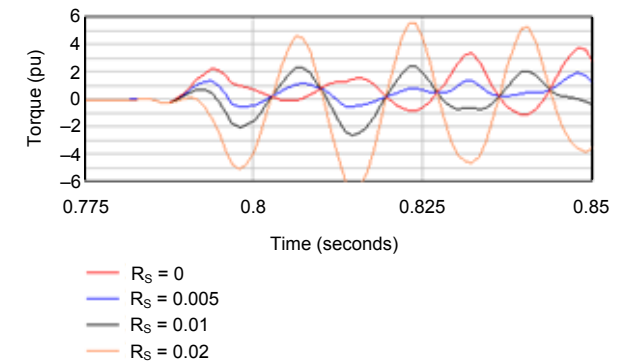

Fig. 26.   Torque vs. R_S

Fig. 27.   A Closer Look at Torque vs. R_S

We know that R_S is not zero because all motors have some stator resistance. Because that plot leads to a large amount of oscillations in the torque signal, we neglect that graph. A value of R_S of 0.02 pu is fairly large for a medium-voltage motor of this size. Because that point also leads to large oscillations in the torque calculation, it is shown more for illustration in Fig. 26 and Fig. 27. A value of R_S at 0.005 pu yields the least amount of oscillation in Fig. 27. If we refine our values of R_S further using data from similar sized machines at similar voltage levels, we can see in Fig. 28 that the variation in torque is much less. Knowing even an approximate value for R_S can help refine the torque calculation.
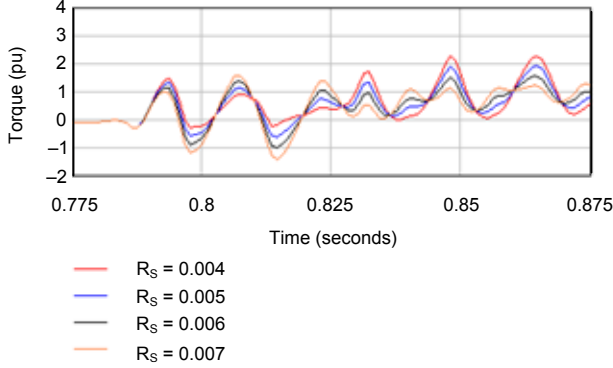

Fig. 28.   Torque With Updated Values for R_S

V.   CONCLUSION

In this paper, we illustrate a method for the calculation of electromagnetic torque directly from motor terminal measurements. We also identify and quantify several potential sources of error. An error in stator resistance produces the most significant errors, but this can be mitigated to a large degree using field measurements and engineering judgement. We demonstrate the method using field data and identify additional problems and solutions associated with data capture. The method is a valuable tool for assessing the impact of all types of transients on the health of a motor.

VI.   APPENDIX

TABLE II
MOTOR MODEL PARAMETERS

Rated VA	746 kW (1,000 hp)
Nominal Voltage (Vnom)	4 kV
Nominal Frequency (fnom)	60 Hz
Stator Resistance (Rs)	0.01117 pu
Stator Inductance (Ls)	0.04832 pu
Rotor Resistance (R′)	0.006 pu
Rotor Inductance (Lr′)	0.04832 pu
Inertia Constant (H)	0.93 seconds
Friction Factor (F)	0.01511 pu
Pole Pairs	2

TABLE III
CT MODEL PARAMETERS

Turns Ratio	300/5
C Rating	C200 and C100
Core Length	0.75 m
Resistive Burden	1 ohm
Maximum Flux Density	1.8 wb/m
Relative Permeability	15000

The following are the equations used in Mathcad® to calculate electromagnetic torque. Note that the equations and process of importing the data is not shown. In the following, k is a sample index and h is the time between samples (1/Fsam). In (15), the division by $\sqrt{3}$ is introduced by using phase-to-phase quantities.

$$IAB_k = IA_k - IB_k \tag{18}$$

$$ICA_k = IC_k - IA_k \tag{19}$$

$$VAB_k = VA_k - VB_k \tag{20}$$

$$VCA_k = VC_k - VA_k \tag{21}$$

$$VABcomp_k = VAB_k - IAB_k \bullet R_S \tag{22}$$

$$VCAcomp_k = VCA_k - ICA_k \bullet R_S \tag{23}$$

$$\text{int } VAB_k = \frac{h}{2} \bullet (VABcomp_k + VABcomp_{k-1}) + \text{int } VAB_{k-1} \tag{24}$$

$$\text{int } VCA_k = \frac{h}{2} \bullet (VCAcomp_k + VCAcomp_{k-1}) + \text{int } VCA_{k-1} \tag{25}$$

$$\psi AB_k = \omega_b \bullet \text{int } VAB_k \tag{26}$$

$$\psi CA_k = \omega_b \bullet \text{int } VCA_k \tag{27}$$

$$DCAB = \frac{1}{3 \bullet spc} \sum_{j=0}^{3 \bullet spc - 1} \psi AB_j \tag{28}$$

$$DCCA = \frac{1}{3 \bullet spc} \sum_{j=0}^{3 \bullet spc - 1} \psi CA_j \tag{29}$$

$$\psi ABm_k = \psi AB_k - DCAB \tag{30}$$

$$\psi CAm_k = \psi CA_k - DCCA \tag{31}$$

$$T_{EM} = \frac{2}{3} \bullet \frac{1}{\sqrt{3}} \bullet (\psi CAm_k \bullet IAB_k - \psi ABm_k \bullet ICA_k) \tag{32}$$

VII.   ACKNOWLEDGMENT

IX. REFERENCES

[1]   J. O. Ojo, V. Ostovic, T. A. Lipo, and J. C. White, "Measurement and Computation of Starting Torque Pulsations of Salient Pole Synchronous Motors," *IEEE Transactions on Energy Conversion*, Vol. 5. Issue 1, March 1990, pp. 176-182.

[2]   P. C. Krause, O. Wasynczuk, and S. D. Sudhoff, *Analysis of Electric Machinery and Drive Systems*. Wiley-IEEE Press, Hoboken, NJ, 2002.

[3]   R. H. Park, "Two-Reaction Theory of Synchronous Machines Generalized Method of Analysis – Part I," *Transactions of the American Institute of Electrical Engineers*, Vol. 48, Issue 3, July 1929, pp. 716-727.

X. BIOGRAPHIES

Dale Finney received his bachelor of engineering degree from Lakehead University and his master of engineering degree from the University of Toronto. He began his career with Ontario Hydro, where he worked as a protection and control engineer. Currently, Mr. Finney is employed as a principal power engineer with Schweitzer Engineering Laboratories, Inc. His areas of interest include generator protection, line protection, and substation automation. Mr. Finney holds more than ten patents and has authored more than 30 papers in the area of power system protection. He is a member of the main committee and vice-chair of the rotating machinery subcommittee of the IEEE Power System Relaying Committee (PSRC). He is a senior member of the IEEE and a registered professional engineer in the province of Nova Scotia.

Derrick Haas graduated from Texas A&M University with a BSEE. He worked as a distribution engineer for CenterPoint Energy in Houston, Texas, until 2006 when he joined Schweitzer Engineering Laboratories, Inc. Mr. Haas has held several titles including field application engineer, senior application engineer, team lead, and his current role of regional technical manager. He is a senior member of the IEEE and involved in the IEEE PSRC.